

# Evaluation of A Soot Modeling Strategy Including Sectional PAH Model and Lagrangian Soot Tracking

Alexis Andre<sup>1</sup>, Nicolas Bertier<sup>1</sup>, Aymeric Boucher<sup>2</sup>, Philippe Villedieu<sup>1</sup>

<sup>1</sup> ONERA, Université de Toulouse, F-31055, Toulouse, France

<sup>2</sup> ONERA, Université Paris Saclay, F-91123, Palaiseau, France

[alexis.andre@onera.fr](mailto:alexis.andre@onera.fr); [nicolas.bertier@onera.fr](mailto:nicolas.bertier@onera.fr)

**Abstract** – Soot prediction has become an important issue due to their impact on health, environment and combustion chamber thermal load. However, soot's evolution mechanisms are still not well understood and stay an open-field of study in computational fluid dynamics. Much soot modeling strategies of various level of complexity exist in literature and most of them having for objective to simulate industrial complexity devices use a very reduce number laminar flames to validate their model. The present work validate a soot modeling strategy, based on a Lagrangian soot tracking associated with a reversible sectional polycyclic aromatic hydrocarbons model, including several variants of gas phase description and soot evolution sub-models, against experimental measurements on a large set of 1D ethylene/air laminar premixed flames. An important variability of results was found and it was shown that some soot modeling strategy could give excellent agreements with experimental data on some flames and vastly overpredict or underpredict soot volume fraction on others. Among all the tested variations, one of them gives a better predictability over all the flames studied even if improvements for its related sub-models should be considered for future work. These results demonstrate the importance of validating one's soot modeling strategy over a sufficiently high number of configurations in order to highlight its main trends and defects.

**Keywords:** ethylene/air, combustion, numerical simulation, ISF, computational fluid dynamics, laminar premixed flames

## 1. Introduction

Soot particles and polycyclic aromatic hydrocarbons (PAH) produced by aircraft engines are an ongoing field of research because of their adverse effects on health and environment as well as on combustion chamber wall thermal load, due to soot radiations. Being able to accurately predict soot formation and evolution is thus an important issue and a challenging task. Critical gaps in the fundamental understanding of soot still exist, in particular for soot nucleation. At the current stage, PAH are thought to be the key intermediate species: PAH of increasing size are formed by reactions between smaller PAH radicals (PAH<sup>\*</sup>) and acetylene until at some size, two PAH react with each other resulting in the inception of the first soot [1]. Then soot interact with the gas phase: growing, by addition of C<sub>2</sub>H<sub>2</sub> or by condensation with PAH and decreasing by oxidation by O<sub>2</sub> or OH. They also interact with each other by collision: when they are young, their liquid like behavior allows them to coalesce while when they age, they regroup themselves by aggregation [2].

Many soot models exist in literature; they can be classified in three categories. Empirical models provide the soot volume fraction through correlations from experimental measurements [3]. They are often used with global chemical kinetics and their predictability is restrained to small ranges of parameters. Semi-empirical models are based on a phenomenological description of the formation and destruction of soot [4]. Unlike empirical models, their source terms of mass do not entirely depend on empirical relations. Although more predictive and widely used in industrial configurations, their physical content is too poor to represent both the complexity of soot chemical evolution and particle dynamics. Detailed models, which are of interest in this paper, are based on a complex description of the gas phase kinetics, relying on a large number of intermediate species and a more complete description of the particle formation and evolution. These models consider soot as particles apart from the gas phase and can take into account their polydispersity [5]. The most used approaches are mainly the sectional methods [6], methods of moment [7], stochastic methods [8] or Lagrangian soot tracking methods [9]. Most soot modeling strategy associated with detailed soot models can be split into three parts: (I) a detailed gas phase kinetics describing the formation of the first aromatic ring and its following growth until a certain size is reached. This part will be referred as “gas phase” in the following. (II) A modeling of larger gaseous PAH not included in the kinetics mechanism, which will be the incipient species. A dimerization method using one or more PAH present in the

gas phase kinetics [5], or a sectional model using lumped PAH [6] may be used. (III) A detailed soot particle model describing soot evolution and dynamics. The present study uses a sectional PAH model coupled with a Lagrangian soot tracking method to describe the evolution of soot particles. This recent approach allows to follow a numerical particle alongside its trajectory in a quasi-deterministic way (a Monte Carlo process is used for collision), and to monitor all its interactions with the surrounding gas phase as well as other particles [5], [9].

When simulating semi-industrial complexity devices, much time consuming issues arise (geometry, mesh, turbulence ...). That is why, most of the time, computational tools aiming to simulate them use only few laminar academic flames to validate their soot modeling strategy. As an example, works of [9] and [6] sharing the same PAH model validate their soot modeling strategy on respectively only one or two laminar configurations. However, seeing the staggering variability of results obtained for different soot modeling strategy, it seems crucial to test one's strategy on more than one or two laminar academic flames before trying more complex configurations. Thus, the objective of the present work is to extend the validation of the present soot modeling strategy to a wide range of flames and equivalent ratios and to test some variations in order to determine which one gives the best global agreement with the experimental data. The 17 flames chosen over four different configurations are ethylene/air premixed-flames which were designated as target by the International Sooting Flame (ISF) workshop [10]. Comparison between simulations for different soot modeling strategy and experimental data for soot volume fraction (fv) are discussed.

## 2. Methodology

The PAH and soot models were implemented in the ONERA CEDRE code [11]. An Arrhenius formulation is used for describing chemical reactions involving PAH and soot. Gas phase and PAH models are solved by the finite volume CHARME solver (Eulerian approach) while soot particle dynamics is computed by the Lagrangian SPARTACCUS solver. A sketch of the whole model is presented in Fig. 1.

### 2.1. Gas Phase Chemistry

Gas phase chemistry is described by a reduced mechanism for ethylene combustion, containing 43 species and 304 reactions. This mechanism, reduced from the skeletal mechanism of Slavinskaya et al. and containing 93 species and 729 reactions [12], was successfully used in previous studies [13], [6], [9].

### 2.2. PAH Modeling

PAH are modeled by the reversible sectional PAH model developed by Eberle et al. [6]. It is composed of three logarithmically scaled sections of PAH and PAH radicals (respectively noted  $PAH_i$  and  $PAH_i^*$ ,  $0 \leq i \leq 2$ ) with a molecular weight ranging from 0.1 kg/mol to 0.8 kg/mol as described in Fig. 2. A soot section  $SOOT_0$  is added for the modeling of incipient soot particles. Thermodynamic and transport properties, atomic composition and viscosity for each section are derived from a well defined set of heavy polycyclic aromatic hydrocarbons.

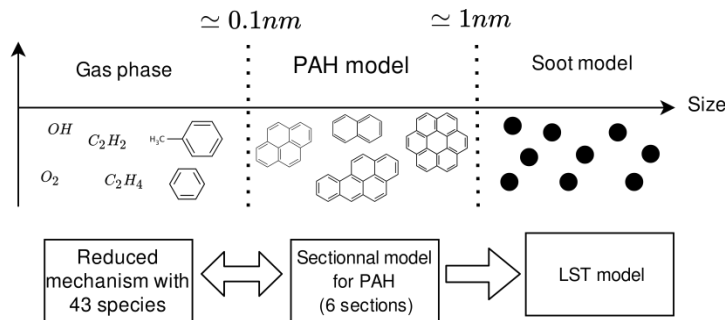


Fig. 1: Sketch of the soot modeling strategy

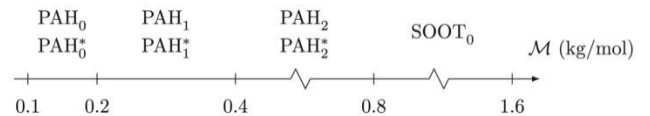
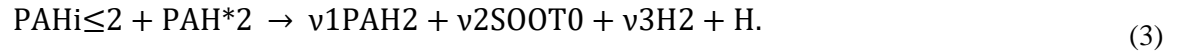


Fig. 2: Definition of  $PAH_i$ ,  $PAH_i^*$  and  $SOOT_0$  sections

Each PAH (for example PAH<sub>0</sub>) is a lumped species that should reproduce all interactions of the PAHs present in its section (between 100 and 200 g/mol for PAH<sub>0</sub>) with the gas phase. To do so, a reaction mechanism for PAH<sub>i</sub> is added, taking into account interactions between gas phase and PAH<sub>i</sub>, surface growth by C<sub>2</sub>H<sub>2</sub> addition, oxidation by O<sub>2</sub> and OH, PAH collisions and dehydrogenation. The collision of PAH<sub>2</sub> or PAH<sub>2</sub>\* with other PAH enables soot nucleation as described in reactions (1)-(3). The stoichiometric coefficients,  $\nu_1$ ,  $\nu_2$  and  $\nu_3$ , computed following the work of Pope et al. [14], ensure elements and mass conservation. All the reaction rates efficiencies are taken from the work of Eberle et al. [6]. The soot nucleation rate, which is the mass production rate of the species SOOT<sub>0</sub>, is obtained as for any other gas species, assuming a molecular weight of  $M_0 = 1.2$  kg/mol. This quantity is sent at each time step for the nucleation of soot particle in the SPARTACCUS solver.



### 2.3. Soot Particle Modeling

Soot particles are modeled by solid spheres with a density equal to  $\rho_s = 1800$  kg/m<sup>3</sup>. At each time step and in each cell, the mass of soot and the number of numerical particles to be created is computed. Incipient soot radius  $r_0$  is equal to  $(3M_0/4\pi N_a \rho_s)^{1/3} = 0.64$  nm, with  $N_a$  the Avogadro number. Each particle created is a numerical particle with a weight  $w_p$  representing many physical ones (up to hundreds of thousands). To prevent having too many soot to follow, a reduction procedure limiting their number at 512 by cells is used [9]. Due to their small diameters (between 1-80 nm), they are considered as tracers of the gas flow. As a consequence, their temperature and velocity are always taken equal to the one of the gas phase. As explained above, soot will evolve through surface growth, oxidation, condensation and collision. Description and expression of the source terms (referred as sub-models in the following) for each phenomenon are described in [9].

Starting from this reference soot modeling strategy, different variations were compared in order to see if an optimal set can be found. First, the soot modeling strategy of [6] share with the present work the gas phase kinetics and the PAH model. However, sub-models for soot evolution are different, in particular for oxidation and surface growth. So, variations with these two sub-models from [6] are tried. An other point is that industrial simulations usually use simple diffusion model with constant Schmidt and Prandlt numbers instead of a complex differential diffusion model (requiring matrix resolution). Indeed, the latter are much more expensive while their effects are not necessarily significant when the turbulence level is high. Therefore, the impact of this difference on the validation test cases is tested in this work. Next, several values for the critical diameter  $d_c$ , which represents the size beyond which a particle is considered to be old and therefore no longer coalesces, can be found in literature [5]. Thus, a variation of its value is studied. Finally, simulations with the complete kinetics mechanism of Slavinskaya et al. [15], with adaptation for the sectional model of PAH but no further reduction, were also performed to check that the reduced mechanism is able to reproduce the same global trends as the complete one. A summary of all the tested variations is presented in Table 1. The reference soot modeling strategy will be named Rd[9]18.

Table 1: Summary of the different model variations

Name	Rd[9]18	Rd[6]18	Rd[6]12	Cd[9]18	Cd[6]18	Cd[6]12	Cs[9]18
Mechanism	reduced	reduced	reduced	complete	complete	complete	complete
Diffusion	differential	differential	differential	differential	differential	differential	simple
Sub-models	[9]	[6]	[6]	[9]	[6]	[6]	[9]
$d_c$ [nm]	18	18	12	18	18	12	18

### 3. Simulations and Analyses

#### 3.1. Test Cases Presentation

The academic ethylene premixed flames simulated in the present study are targets for the ISF workshop as ISF-premixed flames 2, 3, 4 and 6 [10]. Burning in various conditions, these flames share however some characteristics: injection is done by a McKenna type burner, the flow is stabilized downstream by a stabilizing grid or plate and a co-current flow of nitrogen shields the flame from outside perturbations. Operating conditions for the test cases: equivalent ratio  $\Phi$ , pressure P, cold gas temperature  $T_{in}$ , cold gas velocity  $V_{in}$  and molar composition  $X_k$  are reported in Table 1. For all the flames, soot volume fraction data are available (more data should be found on the ISF website and on papers cited within). For the ISF6 configuration, the stabilizing plate, where measurements are done, has a variable height  $H_p = 0.4, 0.45, 0.55, 0.6, 0.7, 0.8, 1.0, 1.2, 1.5$  or  $2.0$  cm. Each height corresponds to a different flame with same operating conditions. The 10 flames of the ISF6 configuration are simulated in this paper.

Table 2: Test cases inlet conditions

Name	$\Phi$ [-]	P [atm]	$T_{in}$ [K]	$V_{in}$ [ $\text{cm}\cdot\text{s}^{-1}$ ]	$X_{\text{C}_2\text{H}_4}$ [%]	$X_{\text{O}_2}$ [%]	$X_{\text{N}_2}$ or $X_{\text{Ar}}$ [%]
ISF2_2.34	2.34	1	298	6.73	14.08	18.05	67.87
ISF2_2.64	2.64	1	298	6.73	15.6	17.73	66.87
ISF2_2.94	2.94	1	298	6.73	17.0	17.04	65.6
ISF3_2.1	2.1	1	298	6.44	12.8	18.3	68.9
ISF3_2.3	2.3	1	298	6.44	13.86	18.09	68.05
ISF4_2.3	2.3	1	298	7.74	13.86	18.09	68.05
ISF4_2.5	2.5	1	298	7.84	14.9	17.87	67.23
ISF6_ $H_p$	2.07	1	473	12.7	16.3	23.7	60.0

#### 3.2. Numerical Modeling

The 2D axisymmetric configurations were simulated in 1D. This simplification often used in literature has been investigated by Xuan and Blanquart [16] for some flames of the ISF database. They show relative differences between 2D and 1D simulation of at most 35%, which is perfectly acceptable in the context of this work. Each flame has its own 1D computational domain and a mesh grid refined within the flame front. For the gas phase, the inlet boundary conditions are deduced from Table 1, atmospheric pressure is imposed at the outlet and symmetry conditions are used elsewhere. For soot numerical particles, all boundary conditions are of “free border” type (no bounces or sticking taken into account). A temperature profile is imposed for each flame, allowing to stabilize the 1D flame and to take into account thermal exchange with the surrounding environment (including radiation). Profiles used for ISF-premixed flames 2, 3 and 4, are the ones suggested by the ISF workshop while for ISF-premixed flame 6 it is obtained (with no radiation effects) with a reference code for 1D flames: Cantera [17]. The temperature profiles are imposed at each time step in each cell by adding a source term in the total energy balance equation.

For the CHARME solver, spatial discretization is performed by second order MUSCL schemes along with an implicit second order Gear method for the temporal integration. The time step is the same for both Eulerian and Lagrangian solver, and the simulated physical time is chosen large enough to reach a steady-state solution.

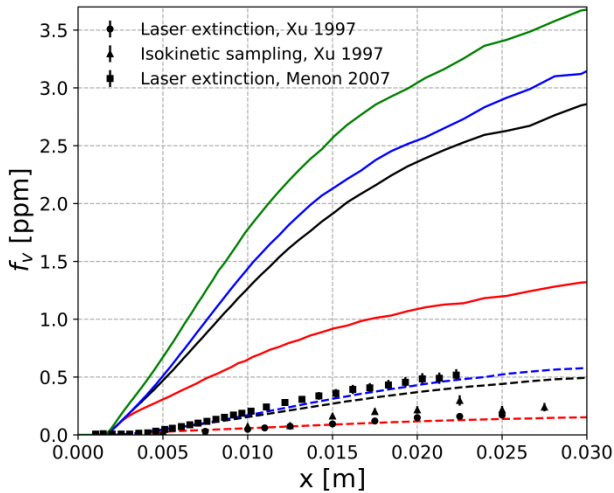
#### 3.3 Results Analysis

Fig. 3 compares the fv with experimental data available for all flames presented in Table 2. A massive variability is observed between the different soot modeling strategies: models can give excellent agreements on some flames and then vastly underestimate (Rd[9]18, Rd[6]18, Rd[6]12) or overpredict (Cs[9]18, Cd[6]18, Rd[6]12) fv. Only Cd[9]18 gives similar trends for all flames. For each height of ISF6, only one experimental measurement for fv is available at the position of the stabilizing plate. This one point measure for each height is presented on the same graph (Fig. 3 (f)) and compared with corresponding simulation results. As suggested by Saggese et al. [18], for heights 0.4 up to 1.2 cm, a spatial shift is applied (between 1.2 and 1.6 mm) to the 1D simulation results to account for the 2D aspiration effect at the stagnation plate. For heights 1.5 and 2.0 cm, a spatial shift of 1.8 mm is taken. No model succeeds to capture the right trend for low

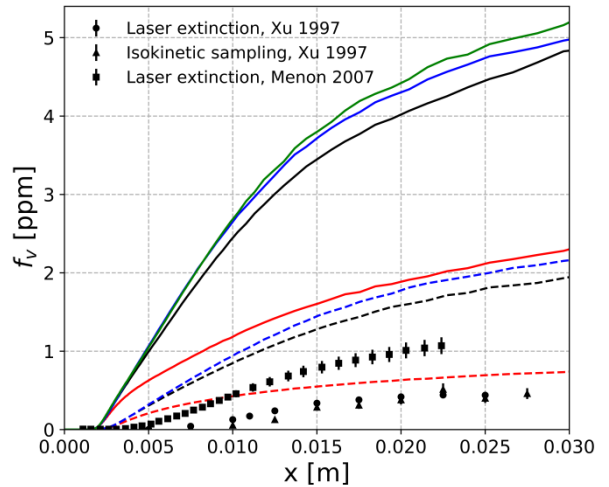
heights. The better tendency is obtained for Cd[9]18, which keeps an increasing profile over all the heights. More investigations would be needed for this configuration in the future.

For almost all the flames studied, a decrease of  $d_c$  leads to a little increase of  $f_v$ . Contrariwise, the influence of  $d_c$  is particularly small and almost no difference is visible for ISF6. As shown in [9], the variation of  $d_c$  is expected to have more impact on the particle sizes than on the soot volume fraction. Moreover, flames studied are short, which prevents the formation of sizeable particles where a change of  $d_c$  could be more impactful.

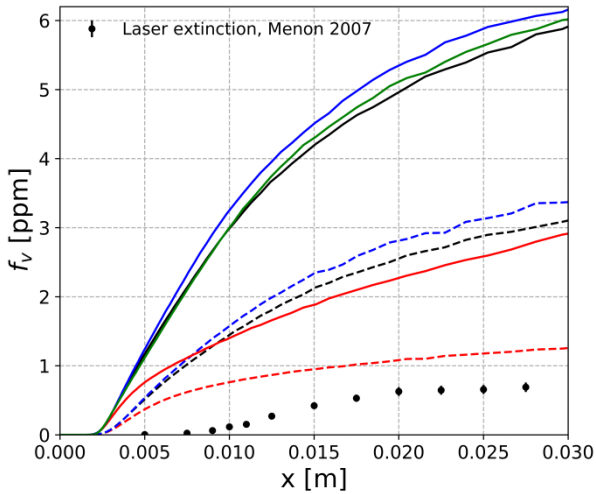
As expected for laminar flames, the impact of the diffusion model is significant. The use of a simplified diffusion model leads to an increase of  $f_v$  for all test cases, in particular for ISF3 with an increase of 100%. Differential diffusion models give better agreement with experimental data and thus their use is mandatory for validations on 1D laminar flames.



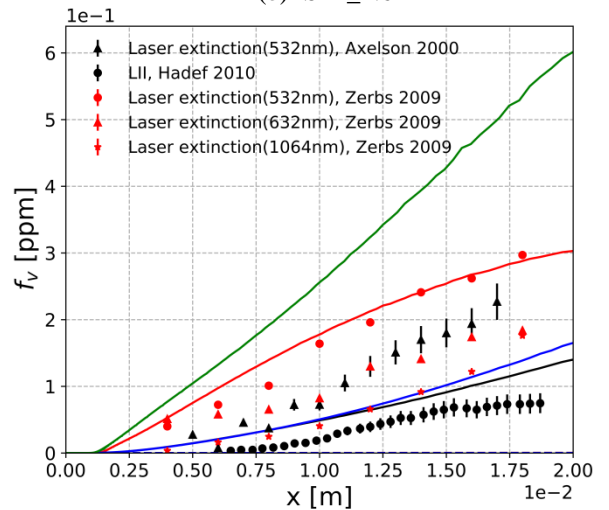
(a) ISF2\_2.34



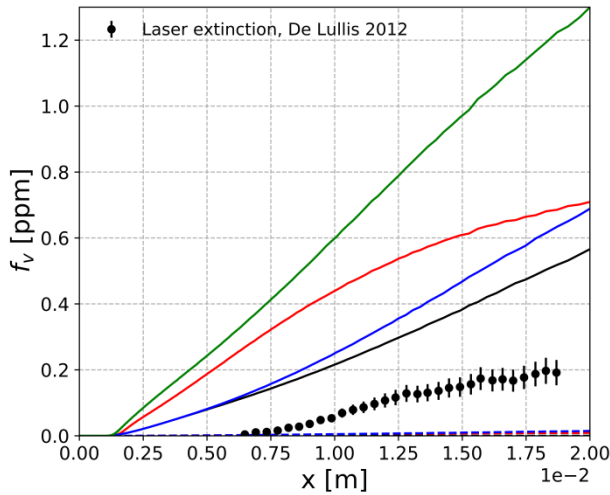
(b) ISF2\_2.64



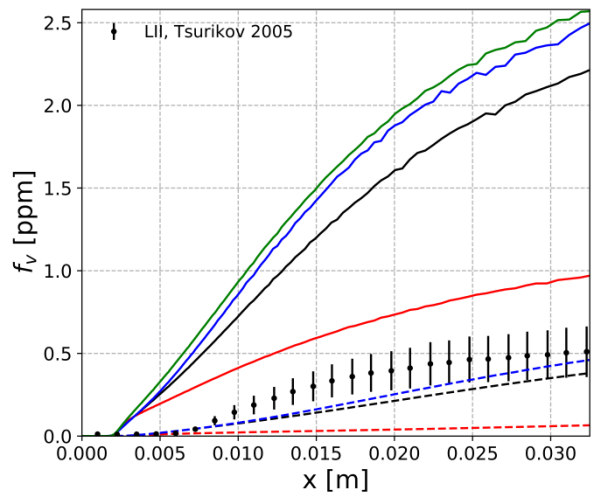
(c) ISF2\_2.94



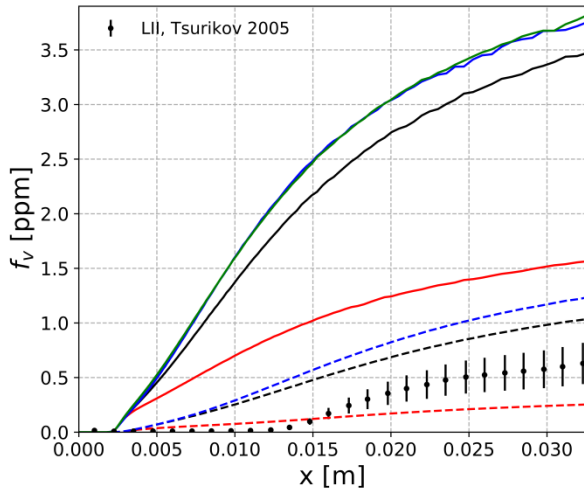
(d) ISF3\_2.1



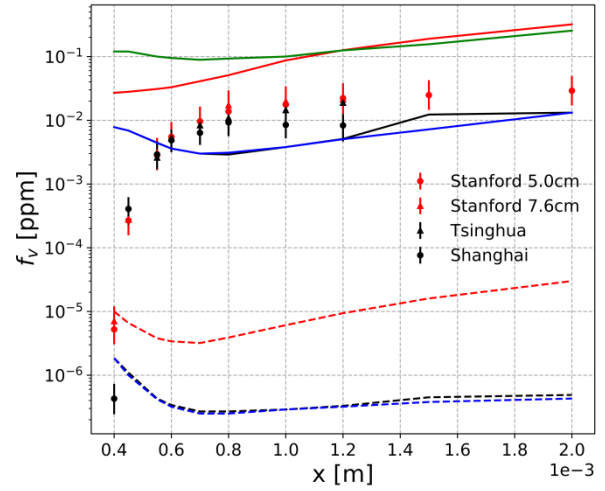
(e) ISF3\_2.3



(f) ISF4\_2.3



(g) ISF4\_2.5



(h) ISF6

Fig. 3: Soot volume fraction along height above the burner for the different test cases and the different variations of the Reference model: Rd[9]18 (◄), Rd[6]18 (◄), Rd[6]12 (◄), Cd[9]18 (◄), Cd[6]18 (◄), Cd[6]182 (◄), Cs[9]18 (◄).

The choice of oxidation and surface growth sub-models for soot has considerable impact on  $f_v$ . No general trend can be seen: for ISF2 and ISF4 soot modeling strategy with sub-models from [9], produce more soot while it is the opposite for ISF3 and ISF6. Nonetheless, contrary to Cd[6]18 model which sometimes over or underpredicts  $f_v$ , the Cd[9]18 model always overpredicts  $f_v$  about a factor five. Thus, this model seems to have a better predictability and, by working on its oxidation and surface growth sub-models, a good agreement for all the flames studied might be reached (even if this improvement might not be effective for all laminar flames that exist in the literature).

Simulations with the complete kinetics mechanism produce more soot for all configurations than with the reduced one. A good agreement with experimental data is obtained for ISF2 and ISF4 with the reduced mechanism and for ISF3 and ISF6 with the complete one. Although the latter overpredicts  $f_v$  for ISF2 and ISF4, the good order of magnitude is reached. However, the reduced kinetics mechanism underpredicts  $f_v$  for ISF3 by two orders of magnitude and ISF6 by four orders of magnitude. As discussed in the next paragraph, the reasons for this lack of soot with the reduced kinetics for these configurations is related to the underprediction at high temperature of important precursors such as benzene compared to the complete mechanism. The soot volume fraction obtained with the reduced kinetics for ISF4\_2.3 and ISF3\_2.3 is vastly different whereas configurations are similar, the biggest difference being the imposed temperature profile. Temperature

profiles imposed for each flame are plotted on Fig. 4. For the sake of clarity, only three representative profiles are shown for ISF6. It appears that all the flames for which simulations with the reduced kinetics widely underpredict  $f_v$ , are the ones with the higher maximum temperature (represented in dashed lines).

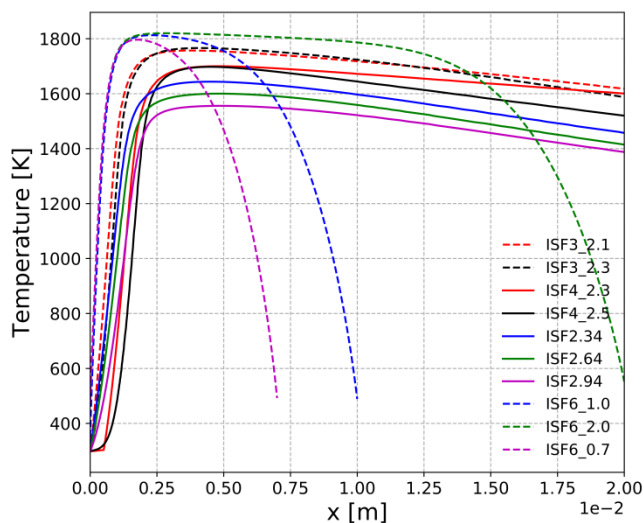


Fig. 4: Imposed temperature profiles of the different test cases

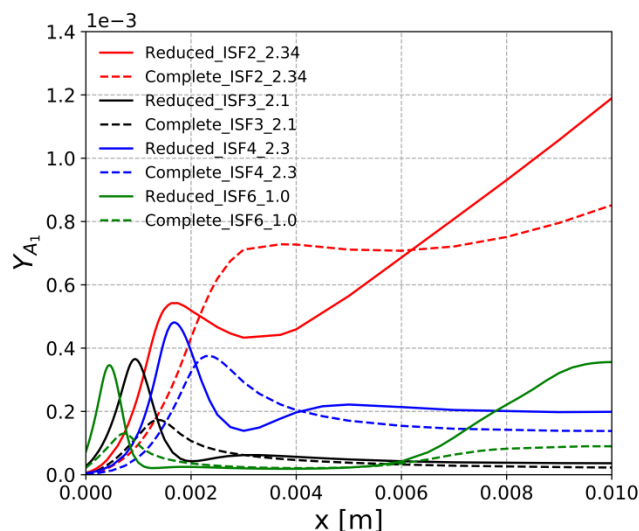


Fig. 5: Profiles of benzene mass fraction for different test cases on Cantera

A comparison of profiles of benzene ( $A_1$ ) mass fraction between the ones obtained with the reduced kinetics mechanism and the ones obtained with the complete mechanism [13], is shown on Fig. 5. These simulations were done on Cantera by imposing the same temperature profiles and initial conditions than in CEDRE. It can be observed that the reduced kinetics underestimate the peak of  $A_1$  by more than 200% for ISF3 and ISF6 (where too little soot is produced) while for ISF2 and ISF4 (where good agreement is obtained for  $f_v$ ) the underestimation is less than 35%. The profiles of benzene were plotted because this species is one of the most important precursors in our mechanism. A lack of benzene will lead to a lack of  $PAH_0$ ,  $PAH_1$  and  $PAH_2$  and thus to a lack of soot. Hence, the large underprediction of soot with the reduced mechanism for ISF3 and ISF6 can be explained by an underprediction, compared to the complete mechanism, of important precursors such as benzene, particularly at high temperature. For future work, a new reduction of the complete mechanism with a better targeting of the level of benzene at high temperature is considered.

## 5. Conclusion

A soot modeling strategy, based on a Lagrangian soot tracking associated with a reversible sectional PAH model, including several variants of gas phase description and soot evolution sub-models, was validated against experimental measurements on a large set of 1D ethylene/air laminar premixed flames. It was shown that contrary to the complete kinetics mechanisms, the reduced one could not reproduce a sufficient high level of soot volume fraction for two configurations out of four. This gap was due to a reduction that did not manage to predict the same amount of essential soot precursors such as  $A_1$  than with the complete mechanism, in particular at high temperatures. Sub-model choices for oxidation and surface growth on soot were found to have a huge impact on  $f_v$ . The Cd[9]18 model seems to give the better predictability over all the flames studied and improvements for its related sub-models can be considered for future work, with the goal to reduce its constant overprediction. More work should also be done on the ISF6 flame to reproduce correct trends for small heights. All these simulations demonstrate the importance of validating the soot modeling strategy over a sufficiently high number of configurations in order to highlight its main defects, which is not always done when

simulations of configurations of industrial interest are considered. At last, a differential diffusion model should always be used for laminar flame simulations to prevent large error (more than 100%) on  $\nu$ .

## Acknowledgements

The authors thank Peter Gerlinger and Martin Grader from DLR for their fruitful discussions. The authors gratefully acknowledge the ANR for funding this project.

## References

- [1] J. T. McKinnon, J. B. Howard, "The roles of PAH and acetylene in soot nucleation and growth," in *Symposium (International) on Combustion*, 1992, vol. 24, pp. 965-971.
- [2] R. Dobbins, "Soot inception temperature and the carbonization rate of precursor particles," *Combustion and Flame*, vol. 130, no. 3, pp. 204-214, 2002.
- [3] J. B. Moss, "Modelling Soot Formation for Turbulent Flame Prediction," in *Soot Formation in Combustion*, H. Bockhorn, Berlin: Springer, 1994, pp. 551-568.
- [4] K. M. Leung, R. P. Lindstedt & W. P. Jones, "Simplified reaction mechanism for soot formation in nonpremixed flames," *Combustion and Flame*, vol. 87, no. 3-4, pp. 289-305, 1991.
- [5] L. Gallen, "Prediction of soot particles in Gas Turbine Combustors using Large Eddy Simulation," Ph.D. dissertation, Dept. Energy and Transfert., INP Toulouse, Toulouse, France, 2020
- [6] C. Eberle, P. Gerlinger & M. Aigner, "A sectional PAH model with reversible PAH chemistry for CFD soot simulations," *Combustion and Flame*, vol. 179, pp. 63-73, 2017.
- [7] M. E. Mueller, G. Blanquart, & H. Pitsch. "Hybrid Method of Moments for modeling soot formation and growth," *Combustion and Flame*, vol. 156, no. 6, pp. 1143-1155, 2009.
- [8] M Balthasar and M Kraft. "A stochastic approach to calculate the particle size distribution function of soot particles in laminarpremixed flames," *Combustion and Flame*, vol. 133, no. 3, pp. 289-298, 2003.
- [9] N. Dellinger, N. Bertier, F. Dupoirieux & G. Legros, "Hybrid Eulerian-Lagrangian method for soot modelling applied to ethylene-air premixed flames," *Energy*, vol. 194, pp. 116858, 2020.
- [10] G. Nathan. (2020, May 28). International Sooting Flame (ISF) Workshop [Online]. Available: <https://www.adelaide.edu.au/cet/isfworkshop/data-sets/laminar-flames>
- [11] A. Refloch, B. Courbet, A. Murrone, P. Villedieu, C. Laurent, P. Gilbank, J. Troyes, L. Tessé, G. Chaineray, J.B. Dargaud, E. Quémerais, F. Vuillot, "CEDRE Software, hal-01182463, pp. 1-10, 2011.
- [12] N. A. Slavinskaya & P. Franck, "A modelling study of aromatic soot precursors formation in laminar methane and ethene flames," *Combustion and Flame*, vol. 156, no. 9, pp. 1705-1722, 2009.
- [13] T. Blacha, M. Domenico, P. Gerlinger & M. Aigner, "A Soot predictions in premixed and non-premixed laminar flames using a sectional approach for PAHs and soot," *Combustion and Flame*, vol. 159, no. 1, pp. 1181-193, 2012.
- [14] C. J. Pope & J. B. Howard, "Simultaneous Particle and Molecule Modeling (SPAMM): An Approach for Combining Sectional Aerosol Equations and Elementary Gas-Phase Reactions," *Aerosol Science and Technology*, vol. 27, no. 1, pp. 73-94, 1997.
- [15] N. A. Slavinskaya, U. Riedel, S. B. Dworkin & M. J. Thomson, "Detailed numerical modeling of PAH formation and growth in non-premixed ethylene and ethane flames," *Combustion and Flame*, vol. 159, no. 3, pp. 979-995, 2012.
- [16] Y. Xuan & G. Blanquart, "Two-dimensional flow effects on soot formation in laminar premixed flames," *Combustion and Flame*, vol. 166, pp. 113-124, 2016.
- [17] D. G. Goodwin, H. K. Moffat & R. L. Speth. Cantera: An object-oriented software toolkit for chemical kinetics, thermodynamics, and transport processes [Online]. Available: <http://www.cantera.org>, 2017. Version 2.3.0.
- [18] C. Saggese, A. Cuoci, A. Frassoldati, S. Ferrario, J. Camacho, H. Wang, T. Faravell, "Probe effects in soot sampling from a burner-stabilized stagnation flame," *Combustion and Flame*, vol. 167, pp. 167-184, 2016.